Computer Assisted Mechanics and Engineering Sciences, 5: 253–266, 1998.

On-line identification of squeeze-film dynamics of multi-mode rotor-bearing system

Zhou Yu
Drive Engineering
Micropolis (S) Pte Ltd, 5 Serangoon North Avenue 5

Lim Tau Meng
Dynamics and Vibration Centre School of MPE, Nanyang Technological University, Nanyang Avenue, Singapore

(Received March 24, 1997)

This paper presents a practical algorithm for on-line parameter identification of squeeze-film bearing of multi-mode rotor-bearing system. The identification procedure is based on modeling each of the bearing pedestal by applying a multi-frequency excitation force on the rotor and frequency transfer function data are used. It suggested that accurate identification coefficients with reduced standard errors can be achieved without resource to full or reduced-order rotor system measurements. The approach can be applied to rotor-bearing system with any degree of complexity and other types of bearing. Simulation and experimental investigation show that the identification algorithm developed in the paper will considerably simplify the measurement and calculation task for testing work in laboratory and industrial environment without any lost of identification accuracy. The experimental results of stiffness and damping characteristics of the squeeze-film bearings for different rotating speed are also presented.

LIST OF SYMBOLS

$\mathbf{C}_{xx}$, etc.	bearing damping coefficients
$\mathbf{C}'_{xx}$, etc.	damping coefficients of pedestal supporting
$\mathbf{G}_{xe}, \mathbf{G}_{ye}$	transfer function
$\mathbf{E}$	error vector
$\mathbf{f}$	external force applied to the estimate pedestal
$\mathbf{K}_{xx}$, etc.	bearing stiffness coefficients
$\mathbf{K}''_{xx}$, etc.	stiffness coefficients of pedestal supporting
m	m bearing pedestal mass
k, n, N	integers
X_e, Y_e	absolute displacement of bearing pedestal in x and y direction respectively
X_{eb}, Y_{eb}	relative displacement of the pedestal to the rotor in x and y direction respectively
$\mathbf{W}_F$	matrix of observations
Φ_F	matrix of unknown coefficients
β_x, β_y	force coefficients
ω	frequency
ω_0	fundamental frequency
$(\bullet)_n^T, (\bullet)_n^i$	real and imaginary components at $\omega = \omega_n$

1. INTRODUCTION

One of the most important factors governing the dynamic behaviors of rotating machinery is the dynamic characteristics of the rotor supports. Adequate knowledge of the support dynamic is

important in analyzing the vibration problems of rotor-bearing system. Squeeze-film bearing is the most commonly used support in rotor-bearing system by incorporating squeeze film damper to control the stability. However, in practical application, the behaviors of squeeze-film bearing cannot be accurately predicted in the design stage. Experimental determination of squeeze-film bearing dynamic coefficients in practical conditions is necessary. Considerable research efforts have been devoted to the problem of bearing dynamic identification. The approaches can be classified into two categories: time domain techniques and frequency domain techniques.

Parameter identification based upon discrete-time modeling and multiple regression analysis [2] are capable of producing good estimations in the ideal case of noise-free measurement and providing the sampling rate is correctly chosen. But in the presence of noise, the error of coefficient identification can become large. However, these errors can be significantly reduced by undertaking parameter identification in the frequency domain [3].

The use of discrete harmonic excitation to identify journal coefficients is well established [11]. The sensitivity of the experimental data with respect to each parameter differs with the excitation frequency. Therefore it is very unlikely that good estimates can be obtained with discrete frequency testing. Nordmann [9] had applied impact force technique to the frequency response functions. The results of the method are better than those of others but facing difficulty in the rapidly decayed response in a well-damped system and the difficulty of exactly reproducing the input disturbance during successive tests. C.R.Burrows [3] used PRBS (pseudo-random binary sequence) as the input form of exciting force, overcoming the problem of impulse and step testing. A least-squares identifier is used to product meaningful coefficient estimates from noisy data and to filter any unwanted harmonic components in the measurement system. But the technique was restricted to the study of a rigid shaft. Later work of [4] took into account of the shaft flexibility. The full model method used by the author to estimate coefficients can obtain very good results, but suffers from tedious measurement task. For the simplified model method proposed by the author, the validity of simplification cannot be justified analytically and constrained to a very special situation.

The frequency-domain techniques presented in this paper by studying each of the bearing pedestals is capable of getting accurate identification results with less measurement and calculation. An on-line frequency domain parameter identification algorithm using frequency transfer function data of the bearing pedestal and an identification test rig were developed. It is shown that the technique developed here provide a much more easy way to reliable on-line parameter identification for rotor-bearing system in a laboratory and in a plant.

2. Identification algorithm

The dynamic characteristics of squeeze-film bearing and pedestal can be represented by the system shown in Fig. 1. The relationship between the force transmitted through the squeeze-film bearings can be usually expressed by the linearised squeeze-film coefficients, i.e. stiffness and damping coefficients $K_{xx}, K_{xy}, K_{yy}, K_{yx}, C_{xx}, C_{xy}, C_{yy}$ and C_{yx} [5]. The bearing pedestal is mounted on flexible foundation which may be expressed as stiffness and damping coefficients $K'_{xx}, K'_{xy}, K'_{yy}, K'_{yx}, C'_{xx}, C'_{xy}, C'_{yy}, C'_{yx}$. The coordinate system oxy is erected with its initial point attached at the center of journal when the pedestal is in static equilibrium position.

The dynamic equation of the system in the x- and y- direction are described as

$$\begin{aligned} m\ddot{Y}_e + C'_{xx}\dot{X}_e + C'_{xy}\dot{Y}_e + K'_{xx}X_e + K'_{xy}Y_e \\ + C_{xx}\dot{X}_{eb} + C'_{xy}\dot{Y}_{eb} + K_{xx}X_{eb} + K_{xy}Y_{eb} = \beta_x f, \end{aligned} \tag{1}$$

$$\begin{aligned} m\ddot{Y}_e + C'_{yy}\dot{Y}_e + C'_{yx}\dot{X}_e + K'_{yy}Y_e + K'_{yx}X_e \\ + C_{yx}\dot{X}_{eb} + C_{yy}\dot{Y}_{eb} + K_{yx}X_{eb} + K_{yy}Y_{eb} = \beta_y f, \end{aligned} \tag{2}$$

where f is the multi-frequency PRBS perturbation force applied to the rotor. The symbols β_x and β_y are denote the force transducer coefficients.

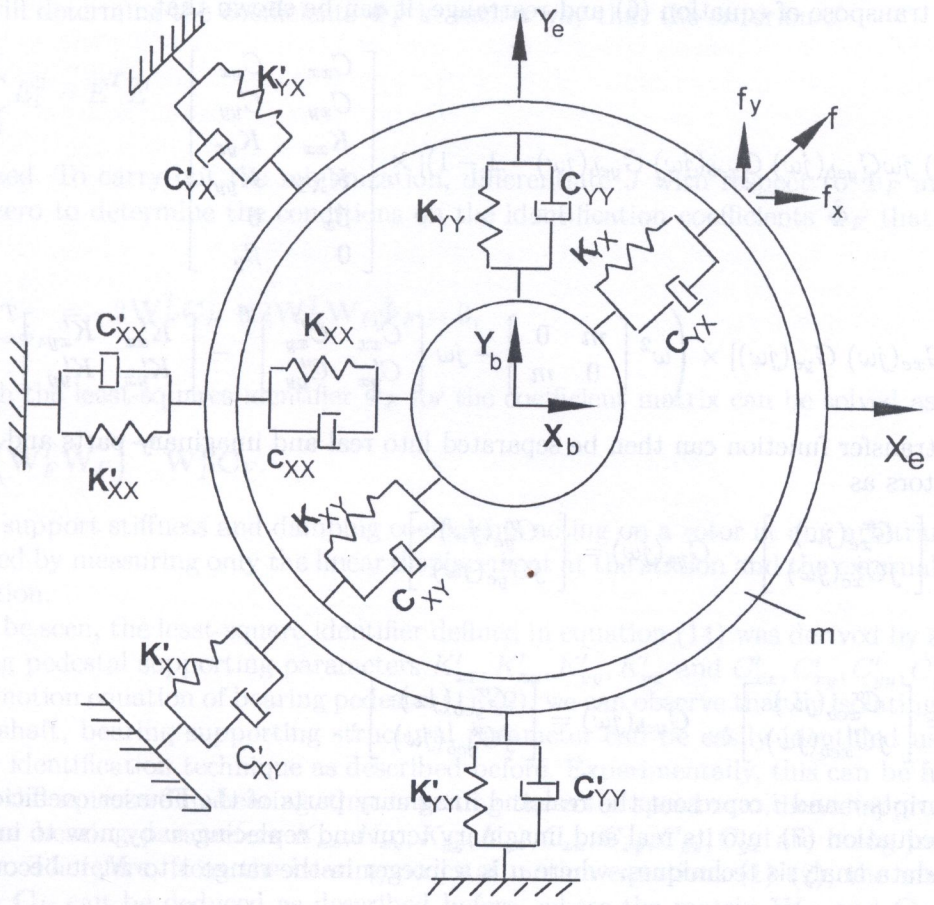

Fig. 1. Bearing pedestal system model

Expressing equation (1) and (2) in the frequency domain and write in matrix form as:

$$\left(-\omega^2\begin{bmatrix} m & 0 \\ 0 & m \end{bmatrix} + j\omega\begin{bmatrix} C'_{xx} & C'_{xy} \\ C'_{yx} & C'_{yy} \end{bmatrix} + \begin{bmatrix} K'_{xx} & K'_{xy} \\ K'_{yx} & K'_{yy} \end{bmatrix}\right)\begin{bmatrix} X_e(j\omega) \\ Y_e(j\omega) \end{bmatrix}$$

$$+\left(j\omega\begin{bmatrix} C_{xx} & C_{xy} \\ C_{yx} & C_{yy} \end{bmatrix} + \begin{bmatrix} K_{xx} & K_{xy} \\ K_{yx} & K_{yy} \end{bmatrix}\right)\begin{bmatrix} X_{eb}(j\omega) \\ Y_{eb}(j\omega) \end{bmatrix} = \begin{bmatrix} \beta_x F(j\omega) \\ \beta_y F(j\omega) \end{bmatrix}. \tag{3}$$

Defining the Fourier coefficients of the transfer function as

$$G_{xeb}(j\omega) = \frac{X_{eb}(j\omega)}{F(j\omega)}, \qquad G_{xe}(j\omega) = \frac{X_e(j\omega)}{F(j\omega)} \tag{4}$$

and

$$G_{yeb}(j\omega) = \frac{Y_{eb}(j\omega)}{F(j\omega)}, \qquad G_{ye}(j\omega) = \frac{Y_e(j\omega)}{F(j\omega)}, \tag{5}$$

where $X_{eb}(j\omega)$, $X_e(j\omega)$, $Y_{eb}(j\omega)$ and $Y_e(j\omega)$ are the displacements and $F(j\omega)$ is the Fourier transform of the applied force.

Equation (4) can then be expressed as

$$\left(-\omega^2\begin{bmatrix} m & 0 \\ 0 & m \end{bmatrix} + j\omega\begin{bmatrix} C'_{xx} & C'_{xy} \\ C'_{yx} & C'_{yy} \end{bmatrix} + \begin{bmatrix} K'_{xx} & K'_{xy} \\ K'_{yx} & K'_{yy} \end{bmatrix}\right)\begin{bmatrix} G_{xe}(j\omega) \\ G_{ye}(j\omega) \end{bmatrix}$$

$$+\left(j\omega\begin{bmatrix} C_{xx} & C_{xy} \\ C_{yx} & C_{yy} \end{bmatrix} + \begin{bmatrix} K_{xx} & K_{xy} \\ K_{yx} & K_{yy} \end{bmatrix}\right)\begin{bmatrix} G_{xeb}(j\omega) \\ G_{yeb}(j\omega) \end{bmatrix} = \begin{bmatrix} \beta_x \\ \beta_y \end{bmatrix}. \tag{6}$$

Taking the transpose of equation (6) and rearrange, it can be shown that

$$[j\omega G_{xeb}(j\omega)\ j\omega G_{yeb}(j\omega)\ G_{xeb}(j\omega)\ G_{yeb}(j\omega) - 1 - 1)] \times \begin{bmatrix} C_{xx} & C_{yx} \\ C_{xy} & C_{yy} \\ K_{xx} & K_{yx} \\ K_{XY} & K_{yy} \\ \beta_x & 0 \\ 0 & \beta_y \end{bmatrix}$$

$$= [G_{xe}(j\omega)\ G_{ye}(j\omega)] \times \left(\omega^2 \begin{bmatrix} m & 0 \\ 0 & m \end{bmatrix} - j\omega \begin{bmatrix} C'_{xx} & C'_{xy} \\ C'_{yx} & C'_{yy} \end{bmatrix}^T - \begin{bmatrix} K'_{xx} & K'_{xy} \\ K'_{yx} & K'_{yy} \end{bmatrix}^T \right). \quad (7)$$

The complex transfer function can then be separated into real and imaginary parts and expressed in column vectors as

$$G_{xe}(j\omega) = \begin{bmatrix} G^r_{xe}(j\omega) \\ jG^i_{xe}(j\omega) \end{bmatrix}, \quad G_{ye}(j\omega) = \begin{bmatrix} G^r_{ye}(j\omega) \\ jG^i_{ye}(j\omega) \end{bmatrix},$$

$$G_{xeb}(j\omega) = \begin{bmatrix} G^r_{xeb}(j\omega) \\ jG^i_{xeb}(j\omega) \end{bmatrix}, \quad G_{yeb}(j\omega) = \begin{bmatrix} G^r_{yeb}(j\omega) \\ jG^i_{yeb}(j\omega) \end{bmatrix}, \quad (8)$$

where superscripts r and i represent the real and imaginary parts of the Fourier coefficient. Then, decomposing equation (7) into its real and imaginary term and replacing w by now to indicate the use of digital data analysis techniques, where n is a integer in the range 1 to N, it becomes:

$$\begin{bmatrix} -n\omega_0 G^i_{xe} & -n\omega_0 G^i_{ye} & G^r_{xeb} & G^r_{yeb} & -1 \\ -n\omega_0 G^r_{xeb} & -n\omega_0 G^r_{yeb} & G^i_{xeb} & G^i_{yeb} & -1 \end{bmatrix} \begin{bmatrix} C_{xx} & C_{yx} \\ C_{xy} & C_{yy} \\ K_{xx} & K_{yx} \\ K_{xy} & K_{yy} \\ \beta_x & \beta_y \end{bmatrix}$$

$$= \begin{bmatrix} (n^2\omega_0^2 m - K'_{xx})G^r_{xe} - K'_{xy}G^r_{ye} + n\omega_0(C'_{xx}G^i_{xe} + C'_{xy}G^i_{ye}) \\ (n^2\omega_0^2 m - K'_{xx})G^i_{xe} - K'_{xy}G^i_{ye} + n\omega_0(C'_{xx}G^r_{xe} + C'_{xy}G^r_{ye}) \end{bmatrix}$$

$$\begin{bmatrix} (n^2\omega_0^2 m - K'_{yy})G^r_{ye} - K'_{yx}G^r_{xe} + n\omega_0(C'_{yy}G^i_{ye} + C'_{yx}G^i_{xe}) \\ (n^2\omega_0^2 m - K'_{yy})G^i_{ye} - K'_{yx}G^i_{xe} + n\omega_0(C'_{yy}G^r_{ye} + C'_{yx}G^r_{xe}) \end{bmatrix}_{n=1,\ldots,N}. \quad (9)$$

Equation (9) can be written in the standard form as

$$\mathbf{W}_F \Phi_F = \mathbf{C}_F, \quad (10)$$

where $\mathbf{W}_F$ is the $2N \times 5$ matrix and $\mathbf{C}_F$ is the $2N \times 2$ matrix containing the Fourier coefficients of the transfer function. Φ_F is the 5×2 matrix of the coefficients to be identified.

Taking into account the error in modeling and random measurement noise, from equation (9) it is generally not possible to determine the set of coefficients $\hat{\Phi}_F$ exactly satisfying all 2N equations (9). An identification of the coefficients Φ_F based on the least-square theory is proposed here. Define an error vector $\mathbf{E} = (E_1, E_2, ..., E_{2N})^T$ as follows:

$$\mathbf{E} = \mathbf{C}_F - \mathbf{W}_F \Phi_F. \quad (11)$$

Now we will determine the coefficients $\hat{\Phi}_F$ in such a way that the criterion J

$$J = \sum_{i=1}^{2N} E_i^2 = \overline{E}^T \overline{E} \tag{12}$$

is minimized. To carry out the minimization, differentiate J with respect to Φ_F and equate the result to zero to determine the conditions on the identification coefficients $\hat{\Phi}_F$ that minimizes J. Thus

$$\left.\frac{\partial J}{\partial \Phi_F}\right|_{\Phi=\hat{\Phi}_F} = -2\mathbf{W}_F^T\mathbf{C}_F + 2\mathbf{W}_F^T\mathbf{W}_F\hat{\Phi}_F = 0, \tag{13}$$

from which the least-squares identifier $\hat{\Phi}_F$ for the coefficient matrix can be solved as:

$$\Phi_F = \left(\mathbf{W}_F^T\mathbf{W}_F\right)^{-1}\mathbf{W}_F^T\mathbf{C}_F. \tag{14}$$

Thus, the support stiffness and damping coefficients acting on a rotor at any arbitrary station can be identified by measuring only the linear displacement at the station and the external force applied to the station.

As can be seen, the least-square identifier defined in equation (14) was derived by assuming that the bearing pedestal supporting parameters $K'_{xx}, K'_{xy}, K'_{yy}, K'_{yx}$ and $C'_{xx}, C'_{xy}, C'_{yy}, C'_{yx}$ are known. From the motion equation of bearing pedestal (1)–(2), we can observe that by isolating bearing from the rotor shaft, bearing supporting structural parameter can be easily identified using the same parameter identification technique as described before. Experimentally, this can be fulfilled by not activating the squeeze-film bearing, that is setting the rotor speed zero, hence approximately zero squeeze-film bearing parameters $K_{xx}, K_{xy}, K_{yy}, K_{yx}, C_{xx}, C_{xy}, C_{yy}, C_{yx}$ are being introduced into the system. Therefore, from the bearing pedestal motion equations (1)–(2), the matrix equation $\mathbf{W}_F\Phi_F = \mathbf{C}_F$ can be deduced as described before, where the matrix $\mathbf{W}_F$ and $\mathbf{C}_F$ contains the Fourier coefficients of the transfer function of bearing pedestal displacement and applied force. The $\hat{\Phi}_F$ matrix contains the unknown bearing pedestal supporting structural parameters, which can be then identified by the least-square algorithm.

3. Experimental investigation

The developed parameter identification procedure has been programmed for practical applications. The adopted identification test installation is shown in Fig. 2. Mathematical model of the testing rotor-bearing system is shown in Fig. 3. The details of the shaft parameters are given in Table 1.

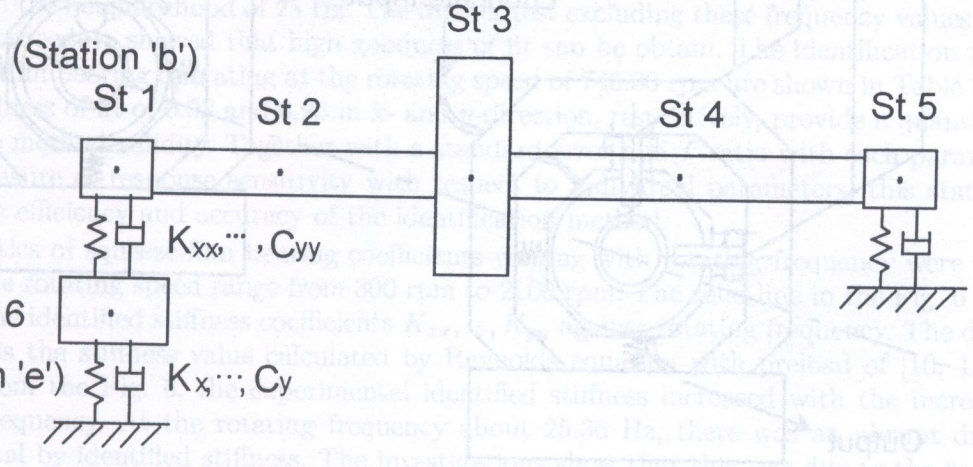

Fig. 2. Mathematical model of the test rotor-bearing system

The shaft is supported on one ball bearing and one testing squeeze-film bearing with both ends carrying one rigid disc. Both bearing pedestal masses are flexibly supported by 4 triangular hooked springs to idealize a point and uncoupled effect of the support system. The spring preload in the y-direction can be adjusted by means of the stud. The lubricant of the testing squeeze-film bearing at one end of the rotor is supplied to the circumferential groove by a pump and discharged to atmosphere at the bearing extremities. The shaft speed is continuously adjustable by means of the variable speed, 2.2Kw electric motor through a belt and pulley system. The system was excited about the equilibrium position at a rotated angle of approximately 45° by a stinger rod attached to a MB Dynamics Model 50 electromagnetic shaker on the ball bearing pedestal. This shaker was supplied with a period of 1.0 sec (fundamental frequency of 1 Hz) and cut-off frequency of 100 Hz

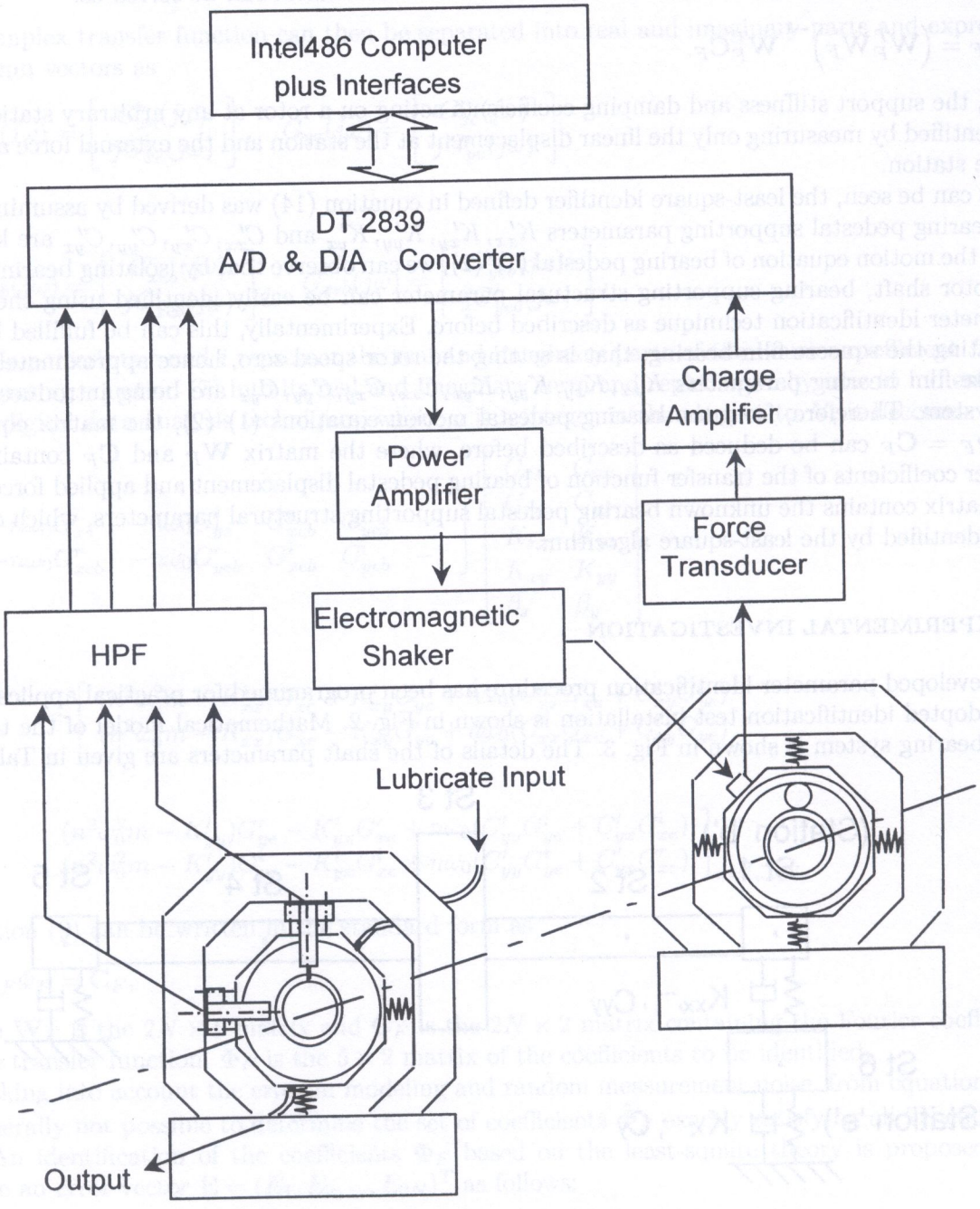

Fig. 3. Diagram of the measurement instruments for squeeze-film bearing

Table 1. Shaft parameters and rigid discs (see Fig. 2.)

Station No.	L mm^{-1}	R mm^{-1}
1	70.0	25.0
2	265.0	25.0
3	20.0	125.0
4	268.0	25.0
5	50.0	25.0
6	–	–
Station No.	Mass kg^{-1}	$I_T \times 10^{-3}(kg\ m^2)^{-1}$
1	0.27489	0.12298
2	1.04064	6.13064
3	1.96350	1.98293
4	1.05243	6.34028
5	0.19635	0.04858
6	1.75838	–

Supporting Stiffness and Dampings of Squeeze-Film Bearing							
$K_{xx}(Nm^{-1})$	79.797E+3	$K_{xy}(Nm^{-1})$	0.0	$K_{yy}(Nm^{-1})$	77.362E+3	$K_{yx}(Nm^{-1})$	0.0
$C_{xx}(Nsm^{-1})$	0.0	$C_{xy}(Nsm^{-1})$	0.0	$C_{yy}(Nsm^{-1})$	0.0	$C_{yx}(Nsm^{-1})$	0.0

Schroeder-phased harmonic signals. The applied force was measured by the squartz load cell, while the journal-to-bearing displacements in both the x- and y-direction were measured using the four eddy current probes of BENTLY NEVADA 7200 series proximity system. The DT2839 AD/DA conversion board was installed in an PC computer to acquire data simultaneously from five channels, as shown in Fig. 3.

The transfer function of the real and imaginary Fourier coefficients for each direction was used instead of the displacement signals considering the repeatability of the sampling digital signal. Averaged signal of 10 periods was also used resulting in the smoothness of the time domain signals and frequency response plot. A typical set of time-domain displacement response at rotating speed 12.383Hz is shown in Fig. 4. After an application of the FFT algorithm to time-domain signal in Fig. 4 the transfer function of the bearing pedestal was determinated by equation (4)-(5) and shown in Fig. 5.

During the signal digital process, the full bandwidth of 1 to 100 Hz was used to determine the bearing coefficients, however, the results yield poor goodness of fits of around 0.5 to 0.8 in both in x- and y-direction. The investigation attributed it to out-of-balance vibration at the rotating speed and oil-whirl in the neighborhood of 25 Hz. The further test excluding these frequency values in the identification procedure showed that high goodness of fit can be obtain. The identification results of the squeeze-film bearing operating at the rotating speed of 743.00 rpm are shown in Table 2. The very high goodness of fit of 0.98 and 0.93 in x- and y-direction, respectively, provide a quantitative measure of the method validity. Together with a standard error and T-ratio with each parameters which is a measure of response sensitivity with respect to individual parameters, this statistical test proved the efficiency and accuracy of the identification method.

Characteristics of squeeze-film bearing coefficients varying with rotating frequency were tested by changing the rotating speed range from 300 rpm to 2100 rpm. The solid line in the Fig. 6 shows the values of the identified stiffness coefficients $K_{xx}, ..., K_{yy}$ against rotating frequency. The dashed line in Fig. 6 is the stiffness value calculated by Reynolds equation with preload of [10, 13]. As can be seen from the Fig. 6, the experimental identified stiffness increased with the increase of the rotating frequency. At the rotating frequency about 25.36 Hz, there was an abrupt drop of the experimental by identified stiffness. The investigations show that this was due to the rotating frequency coincided with the rotor critical frequency which leads to resonance. In this case, the

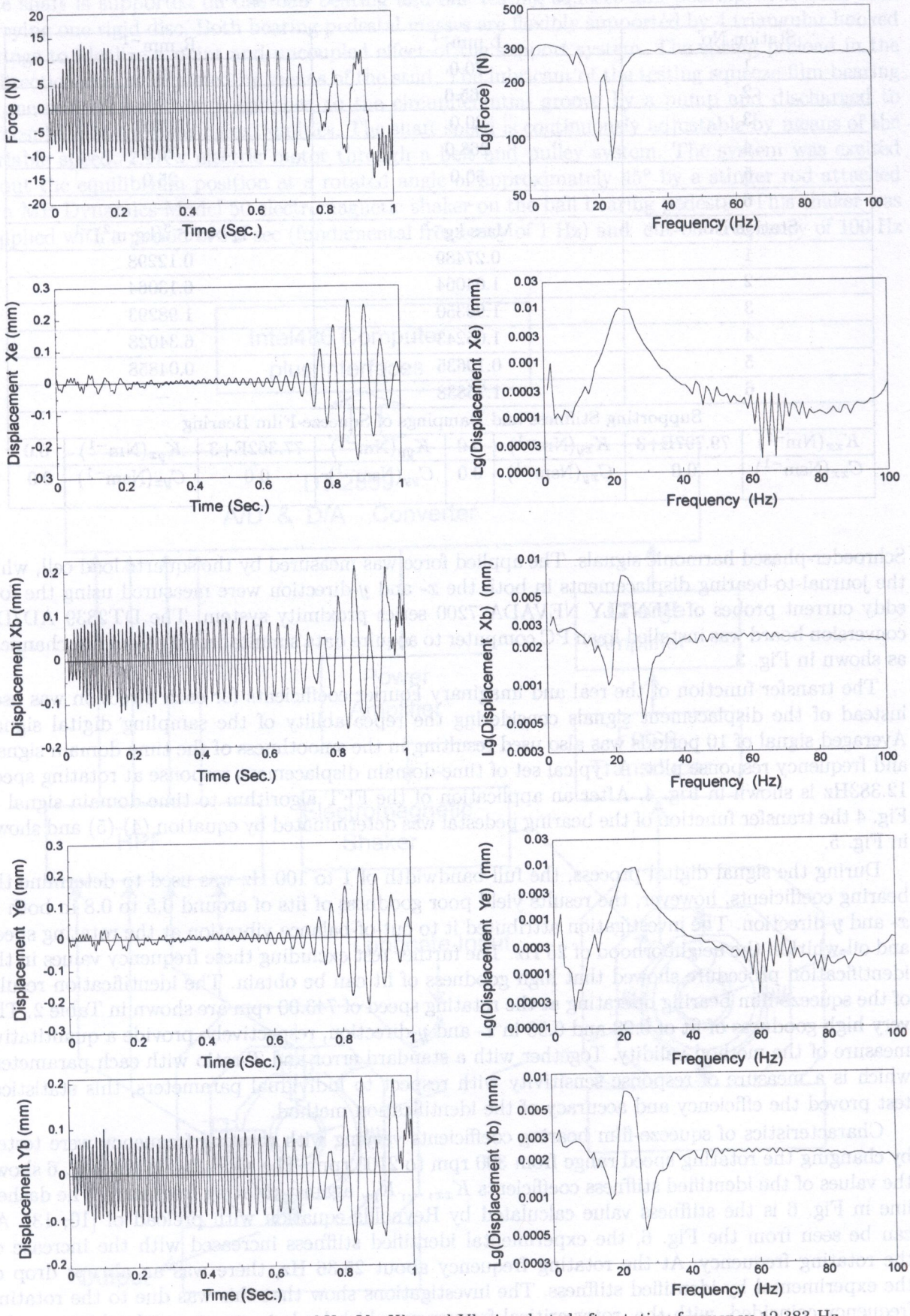

Fig. 4. Time domain plots of Xe, Ye, Xb, and Yb signal at shaft rotating frequency 12.383 Hz

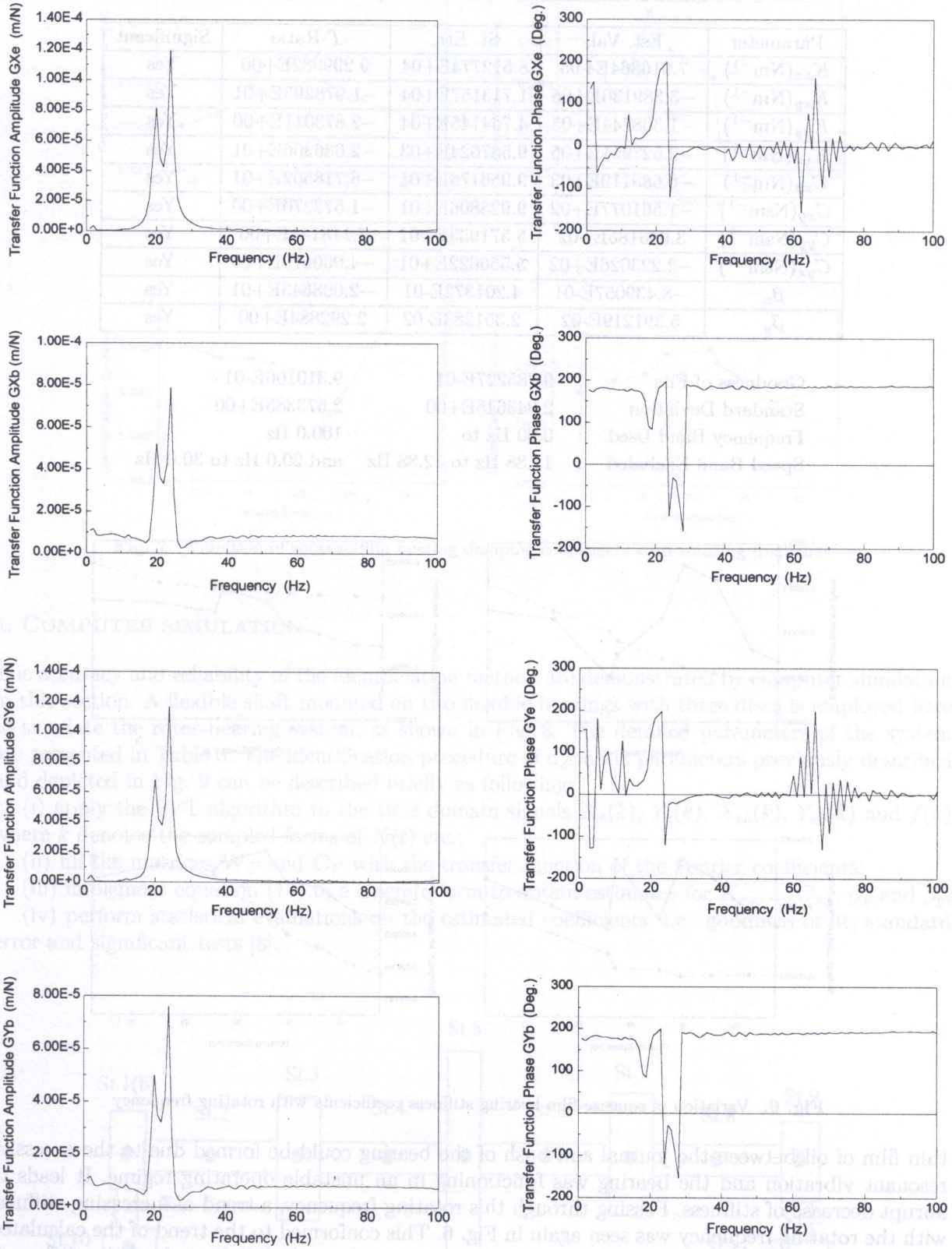

Fig. 5. Amplitude and phase transfer function of Xe/F and Xe/F , Ye/F and Yb/F at shaft rotating frequency 12.383 Hz

Table 2. Identification results from experimenting data

Parameter	Est. Val.	St. Err.	T-Ratio	Significant
$K_{xx}(\mathrm{Nm}^{-1})$	7.916864E+05	8.512774E+04	9.299982E+00	Yes
$K_{xy}(\mathrm{Nm}^{-1})$	−3.389130E+05	1.713157E+04	−1.978295E+01	Yes
$K_{yy}(\mathrm{Nm}^{-1})$	−1.368744E+05	4.764145E+04	−2.873011E+00	Yes
$K_{yx}(\mathrm{Nm}^{-1})$	−2.527951E+05	9.587624E+03	−2.636306E+01	Yes
$C_{xx}(\mathrm{Nm}^{-1})$	−6.689119E+03	9.956176E+01	−6.718562E+01	Yes
$C_{xy}(\mathrm{Nsm}^{-1})$	−1.561077E+02	9.928806E+01	−1.572270E+00	Yes
$C_{yy}(\mathrm{Nsm}^{-1})$	3.966185E+02	5.571933E+01	7.118141E+00	Yes
$C_{yx}(\mathrm{Nsm}^{-1})$	−2.223026E+02	5.556622E+01	−4.000679E+00	Yes
β_x	−8.439057E-01	4.201372E-01	−2.008643E+01	Yes
β_y	5.391219E-02	2.351283E-02	2.292884E+00	Yes

Goodness of Fits	:	9.785227E-01	9.310106E-01
Standard Deviation	:	2.043645E+00	2.573385E+00
Frequency Band Used	:	0.00 Hz to	100.0 Hz
Speed Band Excluded	:	11.88 Hz to 12.88 Hz	and 20.0 Hz to 30.0 Hz

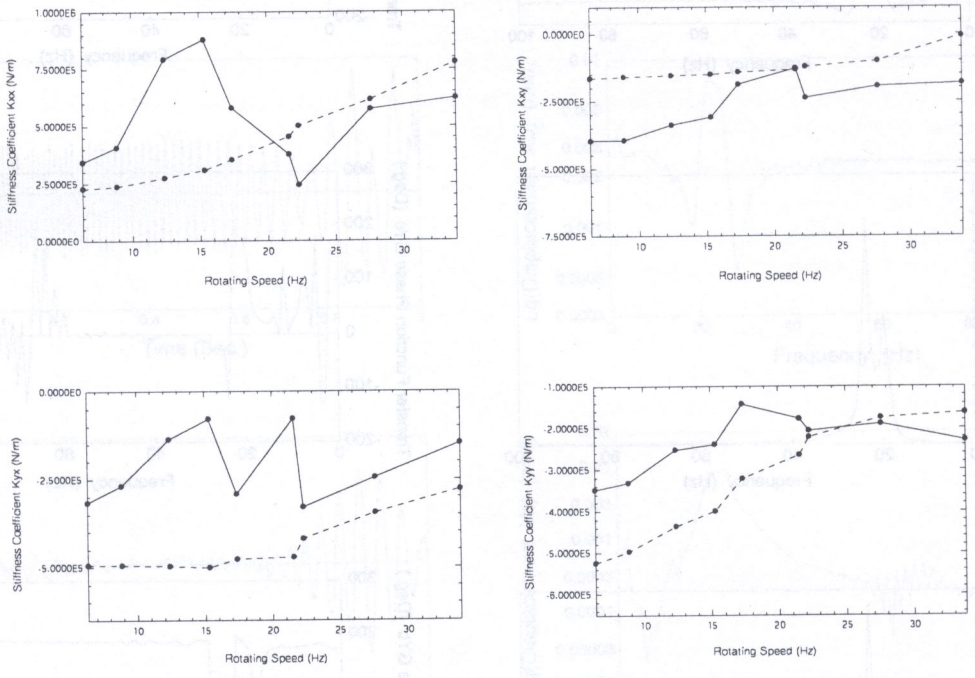

Fig. 6. Variation of squeeze-film bearing stiffness coefficients with rotating frequency

thin film of oil between the journal and bush of the bearing could be formed due to the excessive resonant vibration and the bearing was functioning in an unstable operating regime. It leads to abrupt decrease of stiffness. Passing through this rotating frequency, a trend of increasing stiffness with the rotating frequency was seen again in Fig. 6. This conformed to the trend of the calculated stiffness coefficients. However, the short bearing approximation [14] indicated to the difference between the calculated value and experimentally identified value. Figure 7 shows the identified damping coefficient values $C_{xx}, ..., C_{yy}$ plotted against rotating frequency. As can be seen that the values of the damping were comparatively low and no obvious relationship were shown with the rotating frequency. But at the rotating frequency 25.36Hz, similarly, there was a decrease in damping value due to the resonant vibration.

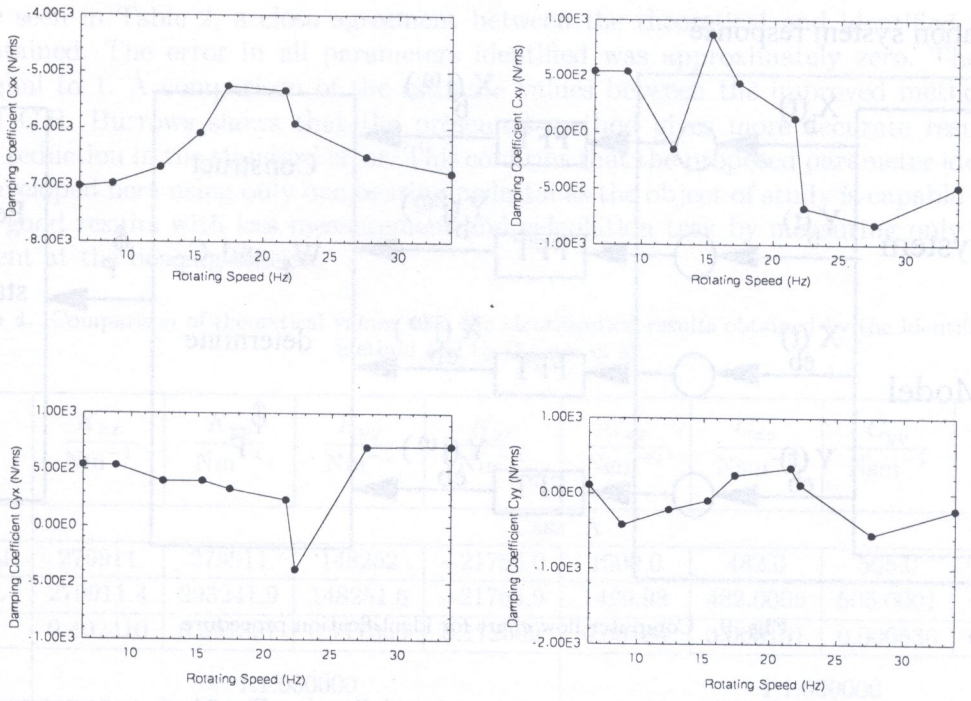

Fig. 7. Variation of squeeze-film bearing damping coefficients with rotating frequency

4. Computer simulation

The accuracy and reliability of the identification method are demonstrated by computer simulation in this section. A flexible shaft mounted on two flexible bearings with three discs is employed here to simulate the rotor-bearing system, as shown in Fig. 8. The detailed parameters of the system are presented in Table 3. The identification procedure of dynamic parameters previously described and depicted in Fig. 9 can be described briefly as following:

(i) apply the FFT algorithm to the time domain signals $X_e(k)$, $Y_e(k)$, $X_{eb}(k)$, $Y_{eb}(k)$ and $f(k)$ where k denotes the sampled forms of $X(t)$ etc.;

(ii) fill the matrices $\mathbf{W}_F$ and $\mathbf{C}_F$ with the transfer function of the Fourier coefficients;

(iii) implement equation (14) in a discrete form to obtain estimates for $K_{xx}, ..., C_{xx}$, β_x and β_y;

(iv) perform statistical evaluations on the estimated coefficients, i.e.. goodness of fit, standard error and significant tests [8].

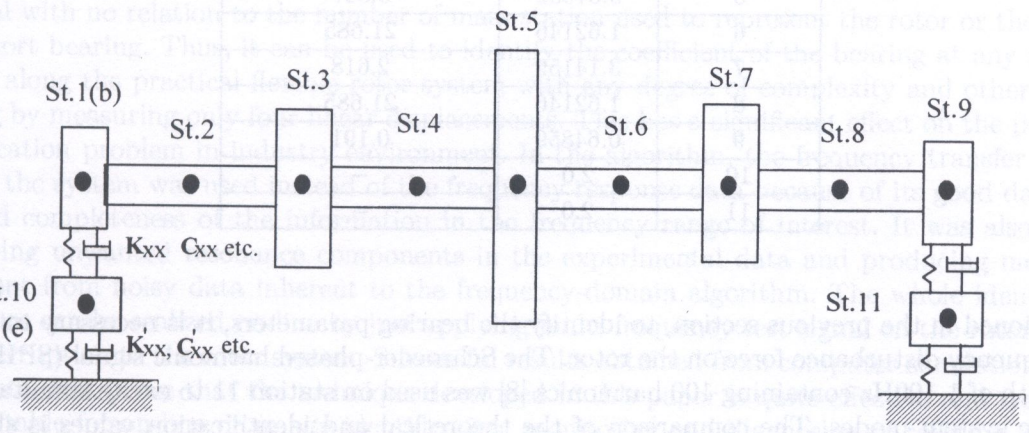

Fig. 8. Mathematical model of a flexible rotor-bearing system

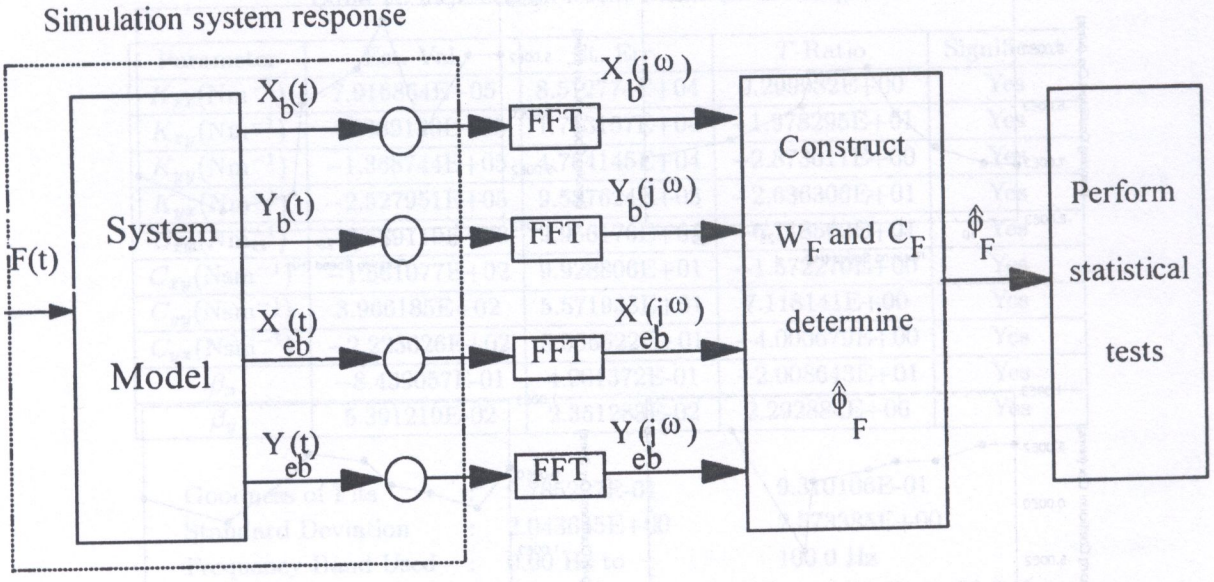

Fig. 9. Computer flow chart for identification procedure

Table 3. Shaft parameters and rigid discs (see Fig. 8.)

Station No.	L mm^{-1}	R mm^{-1}
1	40.0	50.8
2	400.0	25.4
3	50.0	100.0
4	400.0	25.4
5	35.0	126.4
6	400.0	25.4
7	50.0	100.0
8	400.0	25.4
9	40.0	50.8
Station No.	Mass Kg^{-1}	$I_T \times 10^{-3}$ (Kg m^2)$^{-1}$
1	0.64859	0.191
2	1.62146	21.685
3	3.14159	2.618
4	1.62146	21.685
5	3.51352	3.867
6	1.62146	21.685
7	3.14159	2.618
8	1.62146	21.685
9	0.64859	0.191
10	2.0	–
11	2.0	–

As mentioned in the previous section, to identify the bearing parameters, it is necessary to apply a multifrequency disturbance force on the rotor. The Schroeder-phased harmonic signal (SPHS) with bandwidth of 1-100Hz containing 100 harmonics [8] was used on station 11 to excite simultaneously all of the system modes. The comparison of the theoretical and identification values is shown in Table 4. The results obtained by C.R. Burrows [6] using full model are also listed in Table 4.

As can be seen in Table 2, a close agreement between the theoretical and identified coefficients can be obtained. The error in all parameters identified was approximately zero. The goodness of fit is equal to 1. A comparison of the estimate values between the improved method and the method of C.R. Burrows shows that the presented method gives more accurate results with a significant reduction in the standard error. This confirms that the proposed parameter identification method developed here using only one bearing pedestal as the object of study is capable to produce extremely good results with less measurement and calculation task by measuring only four linear displacement at the bearing station.

Table 4. Comparison of theoretical values with the identification results obtained by the identification method and by Burrow et al

Para-meter	$\frac{K_{xx}}{\mathrm{Nm}^{-1}}$	$\frac{K_{xy}}{\mathrm{Nm}^{-1}}$	$\frac{K_{yy}}{\mathrm{Nm}^{-1}}$	$\frac{K_{yx}}{\mathrm{Nm}^{-1}}$	$\frac{C_{xx}}{\mathrm{Nsm}^{-1}}$	$\frac{C_{xy}}{\mathrm{Nsm}^{-1}}$	$\frac{C_{yy}}{\mathrm{Nsm}^{-1}}$	$\frac{C_{yx}}{\mathrm{Nsm}^{-1}}$
	Case A							
Theo.Val.	279911	279911	148252	−21756.0	1500.0	482.0	505.0	482.0
Est.Val.	279911.4	293241.9	148251.6	−21755.9	1499.98	482.0005	505.0001	481.9998
St.Err.	0.402410	0.591307	0.117060	0.172009	0.00184	0.003101	0.000536	0.000902
$\overline{R}^2$	1:1.000000				1:1.000000			
	Case B							
Est.Val.	279910.9	293242.6	148250.8	−21755.3	1499.99	482.0011	504.9978	482.0005
St.Err.	0.459933	0.663494	0.376577	0.261043	0.002147	0.00340	0.001930	0.001218
$\overline{R}^2$	1:1.000000				1:1.000000			

Case A Estimation by using the improved identification method.
Case B Estimation by using the method of C.R. Burrows [6].
$\overline{R}^2$ Denotes goodness of fit.

5. Conclusion

In this paper, a frequency-domain technique for identification of squeeze-film bearing coefficients for on-line application has been developed. Unlike the previously described frequency-domain algorithm for squeeze-film bearing coefficient identification, which can produce meaningful results from noisy data compared with the time-domain algorithm, but suffering from large measurement and calculation task in on-line identification of laboratory and industry environment, the on-line frequency-domain identification technique presented here can be carried out on one of the bearing pedestal with no relation to the number of mass station used to represent the rotor or the number of support bearing. Thus, it can be used to identify the coefficient of the bearing at any arbitrary station along the practical flexible rotor system with any degree of complexity and other types of bearing by measuring only four linear displacements. This has a significant effect on the parameter identification problem in industry environment. In the algorithm, the frequency transfer function data of the system was used instead of the frequency response data because of its good data quantity and completeness of the information in the frequency range of interest. It was also capable of filtering unwanted resonance components in the experimental data and producing meaningful coefficient from noisy data inherent to the frequency-domain algorithm. The whole identification procedure can be realized on-line by just applying multi-frequency test signal on the rotor without any interruption to the rotor system. Successful results obtained from computer simulation and experimental test prove that the technique developed in this paper is quite effective and reasonable. It is suitable for on-line or *in-situ* identification, monitoring and diagnosing of rotating system in industry environment.

REFERENCES

[1] K. Brockwell and W. Dmochowski. Experimental determination of the journal oil film coefficients by the method of selective vibration orbits. *ASME, Design Engineering Division*, **18** (1): 251–259, 1989.

[2] C.R.. Burrows and R.. Stanway. Identification of squeeze-film bearing characteristics. *Journal of Dynamic System, Measurement and Control, ASME Trans.*, **99**: 167–173, 1977.

[3] C.R.. Burrows and M.N. Sahinkaya. Frequency-domain estimation of linearised journal coefficients. *Journal of Lubrication Technology, ASME Trans.*, **104**: 210–215, 1982.

[4] C.R.. Burrows and M.N. Sahinkaya. Parameter estimation of multi-mode rotor-bearing systems. *Proc. R. Soc. Lond.*, **A379**: 367–387, 1982.

[5] M.J. Goodwin. *Dynamic of Rotor-Bearing System*. Unwin Hyman Ltd., London, UK 1989.

[6] J. Ellis, J.B. Roberts and M.D. Ramli. The experimental determination of squeeze-film dynamic coefficients using the state variable filter method of parametric identification. *Trans. ASME, Journal of Tribology*, **111**: 252–259, 1989.

[7] J.M. Krodkiewski and J. Dino. Theory and experiment on a method for on-site identification of configurations of multi-bearing rotor system. *Journal of Sound and Vibration*, **164**(2): 281–293, 1993.

[8] T.M. Lim. The development of a simple magnetic bearing for vibration control. Ph.D. Thesis, University of Strathclyde, UK, 1987.

[9] R.. Nordmann and K. Schollhorn. Identification of stiffness and damping coefficients of squeeze-film bearings by means of the impact method. *Vibration in Rotating Machinery, I Mech.* E, Paper C285/80, 231–238, 1980.

[10] O. Reynolds. On the theory of lubrication and its application to Mr. Beauchamp tower's experiments, including an experimental determination of the viscosity of olive oil. *Phil. Trans. Roy. Soc.*, **177**(1): 157–235, London, 1986.

[11] J.B. Roberts, R.. Holmes and P.J. Mason. Estimation of squeeze-film damping and inertial coefficients from experimental free-decay data. *Proc. Ins. Mech. Engrs*, Part C, 200(C2), 123–133, 1986.

[12] J. Tonnesn. Experimental parameter study of a squeeze-film bearing. *ASME Journal of Lubrication Technology*, **93**: 143–153, 1971.

[13] Z.M. Zhang, J. Zhu J. *Rotor Bearing Lubrication Theory*. Xi'an Jiaotong Univ. Publishing Ltd., China, 1982.

[14] R.. Holmes and M. Dede. Dynamic pressure determinations in a squeeze-film damper. *Mech E Conf. On Vibration in Rotating Machinery*, Paper C260/80, 71–75, York, 1980.